

Exciton-polariton dynamics and photoluminescence line shapes in cadmium telluride

Donald E. Cooper and P. R. Newman

Rockwell International Science Center, P.O. Box 1085, Thousand Oaks, California 91360

(Received 14 November 1988)

Time-resolved and steady-state photoluminescence (PL) data on excitonic polaritons in CdTe are presented and analyzed in terms of polariton formation, transport, and relaxation processes. The sample-to-sample variation in the polariton line shape and the shapes of the various polariton phonon sidebands indicate that there is substantial polariton emission from below the bottleneck region, which shows that transport effects dominate the polariton line shape. Time-resolved PL data from the polariton band show that both formation and decay rates vary with time and k state, producing complex polariton decay waveforms. Polariton formation at the bottom of the band persists for up to 3 ns after optical excitation. Bound-exciton lifetimes can be extracted from the bound-exciton PL decay waveforms if the time dependence of the binding-polariton population is known. These results are compared with previous experimental and theoretical studies of polariton dynamics.

I. INTRODUCTION

Excitonic polaritons have been of theoretical and experimental interest since the first theoretical treatment about 30 years ago.^{1,2} The strong coupling between photons and excitons in a direct-band-gap semiconductor such as CdTe produces polariton states that are superpositions of excitons and photons. The polariton dispersion curve for CdTe is shown in Fig. 1. The pure exciton and photon states mix and form the upper and lower polariton branches, which can be calculated from the dispersion relation³

$$\left(\frac{\hbar kc}{E}\right)^2 = \epsilon \left[1 + \frac{2E_{LT}E_T^2(k)}{E_T(k)[E_T^2(k) - E^2]} \right], \quad (1)$$

where the transverse exciton energy $E_T(k)$ is determined by the exciton mass M and the zone-center transverse exciton energy E_T ,

$$E_T(k) = E_T + \frac{\hbar^2 k^2}{2M}, \quad (2)$$

and ϵ is the background dielectric constant, and E_{LT} is the longitudinal-transverse exciton splitting. The polariton dispersion curve in Fig. 1 was calculated from parameters measured using resonant Brillouin scattering (RBS) on CdTe:⁴

$$E_T = 1.5954 \text{ eV},$$

$$E_{LT} = 0.4 \text{ meV},$$

$$M = 2.4m_e,$$

$$\epsilon = 10.4.$$

RBS directly probes the polariton dispersion, so the curves shown in Fig. 1 should be quite accurate. Figure 1(b) shows the group velocity as a function of energy for the lower polariton branch, which is simply the derivative of the dispersion curve.

Polariton effects have been observed experimentally through reflectivity, transmission, and luminescence,⁵ and with particular success by Raman spectroscopy.⁶ This work has made it possible to measure experimentally the polariton dispersion curves and to verify that the lowest electronic excited state of the intrinsic crystal is the polariton state.

The interpretation of the line shape of the polariton photoluminescence (PL) band has recently aroused considerable controversy.⁷⁻¹² The emission of a photon by a polariton is fundamentally different from corresponding processes associated with most excited states, since electromagnetic energy resonant with the polariton band travels through the crystal as a polariton. Thus in order for a polariton in the interior of a crystal to emit a photon, it must first migrate to the crystal surface, where it can be converted to a photon and thus radiated. In this paper we will present experimentally observed polariton PL spectra in CdTe, and show that transport processes

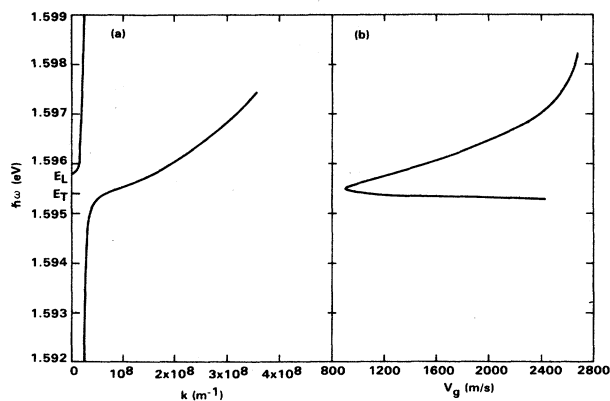


FIG. 1. (a) Dispersion relation for excitonic polaritons in CdTe, calculated from experimentally determined parameters (Ref. 4). (b) The polariton group velocity (V_g , bottom scale) on the lower branch as a function of polariton energy (left scale).

play a major role in determining the shape of the polariton line.

There are also unanswered questions concerning the dynamics of polaritons. Free excitons created well above the polariton region relax by emitting phonons. As the polariton relaxes toward the "knee" region of the dispersion curve [Fig. 1(a)], the rate of phonon emission decreases, forming a "bottleneck"¹³ which allows the polariton population to reach a thermal equilibrium with the lattice temperature. Finally, the polaritons decay through radiation and trapping at impurity sites. The development of ultrafast lasers and experimental techniques¹⁴ has allowed the direct experimental observation of this process,^{3,15-18} but specific mechanisms governing polariton relaxation remain unclear. In this paper we present data on polariton relaxation in CdTe and show that delayed polariton formation and free-carrier relaxation play important roles in the cooling of the polariton population.

Bound-exciton lines are very prominent in the near-band-edge PL spectra of many semiconductors.¹⁹ The temporal dependence of the bound-exciton populations are largely determined by the polariton population dynamics. We will show that the bound-exciton lifetimes can be extracted from the data, provided that the polariton population dynamics are known.

Cadmium telluride is useful as a substrate for fabrication of ir detectors based on $\text{Hg}_{1-x}\text{Cd}_x\text{Te}$, and for this reason considerable effort has been expended in growing pure and defect-free crystals. The defect and impurity concentrations of the CdTe crystals we have studied vary considerably,²⁰ and only the better samples show substantial polariton emission. Many papers have been written on the PL spectra of CdTe,²¹⁻²⁵ and most are directed toward identifying impurities and defects responsible for the various spectral features. We believe ours is the first detailed study of the polariton dynamics and spectral line shapes in CdTe at low temperatures.

The remainder of this paper is organized into sections that consider a specific type of data. Section III presents the near-band-edge steady-state PL spectrum of a high-quality sample of bulk CdTe. Section IV is a detailed examination of steady-state polariton line shapes resulting from various radiative mechanisms. Section V deals with the time-resolved PL of the polariton band, and considers the questions of polariton formation, relaxation, and decay. Section VI presents PL decays for bound excitons, and shows how the bound-exciton decay lifetime can be measured despite the complex polariton dynamics.

II. EXPERIMENT

Cadmium telluride samples from a variety of sources were examined, and the samples with the greatest amount of polariton emission were selected for this study. Samples were in the form of (111)-oriented wafers. To correct the as-grown Te-rich stoichiometry, the samples were annealed for 3 d at 600°C in an equilibrium Cd atmosphere. Hall measurements on the highest-purity sample (no. 1) were not possible because Ohmic contacts could not be formed—this is indicative of high purity. Following the

Cd anneal, about 20 μm of material was removed from the surface using a 2% Br/CH₃OH etchant for 5 min. Before the samples were mounted in the experimental Dewar they were subjected to a brief clean-up etch in 0.5% Br/CH₃OH. During the experiment the samples were immersed in superfluid liquid helium ($T < 2.2$ K).

To obtain steady-state PL spectra, the samples were illuminated with a chopped 0.5-mW He-Ne laser (632.8 nm) focused with a 10-cm-focal-length cylindrical lens. The resulting luminescence was dispersed in a 3/4-m double monochromator and detected by a microchannel-plate photomultiplier (PMT). The signal was processed with a lock-in amplifier and displayed and stored on a microcomputer.

For the time-resolved PL experiment, the exciting laser was a synch-pumped mode-locked cavity-dumped Rhodamine-6G dye laser operating at 600 nm and 4 MHz. A red (long-wavelength passing) filter was placed over the monochromator slits to reject scattered laser excitation light. The technique of time-correlated single-photon counting¹⁴ was used to obtain PL decay data. The same monochromator and detection system was used. The instrument temporal response was approximately 250 ps full width at half maximum (FWHM).

III. STEADY-STATE PHOTOLUMINESCENCE SPECTRA OF CdTe

The near-band-edge cw PL spectrum of a high-quality (low defect and impurity concentration) CdTe sample (no. 1) is shown in Fig. 2. All the features in this spectrum have been assigned previously,^{21,22} and only the polariton and bound-exciton lines will be discussed here. The highest-energy emission is from the excitonic polariton (X) at 1.59 eV. The line shape of this feature is directly affected by the polaritonic nature of the exciton, and there is considerable variation in line shape from sample to sample (Sec. IV below). Polaritons also relax through luminescence with the simultaneous emission of a LO phonon and a photon of about 1.575 eV (the X -LO feature). This process produces a polariton that is mostly photonlike, which readily propagates through the sample to the surface. Although the magnitude of the X -LO emission varies from sample to sample, the line shape does not. Despite the fact that the polariton dispersion

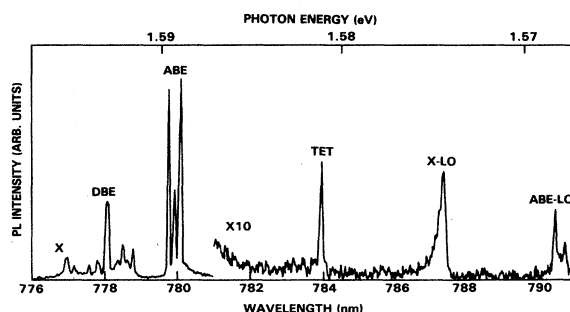


FIG. 2. The near-band-edge PL spectrum of CdTe sample 1, dominated by emission associated with the recombination of excitons.

(Fig. 1) has no energy gap below E_T , the slow (nanosecond time scale) relaxation through the bottleneck region allows a quasistationary thermal distribution (in equilibrium with the lattice temperature) to form above the bottleneck.^{3,15} This quasithermal equilibrium is what determines the line shape of the X -LO band, and the band broadens toward higher energies at higher temperatures. In Sec. V we analyze the temporal behavior of different k states in the polariton band by observing the buildup and decay of PL at various wavelengths across the X -LO band.

The sharp, prominent lines in the PL spectrum are due to bound excitons, with the principal donor-bound exciton (DBE) at 1.593 eV and the acceptor-bound exciton (ABE) near 1.589 eV.²¹⁻²⁵ The energy of the ABE depends on the specific type of acceptor,²⁵ and thus it is useful for identifying impurities. This sample shows three ABE peaks assigned (in order of decreasing energy) to copper, sodium or lithium, and phosphorus. The feature at 1.581 eV is due to the two-electron transition (TET) involving the recombination of excitons bound to neutral donors resulting in an excited neutral donor as the final state.²¹

Figure 2 shows that the bound-exciton emission is much greater than the total polariton emission. Oscillator strengths of bound excitons are very large,^{19,26,27} and so the quantum yield for bound-exciton luminescence is nearly unity. Thus the bound-exciton luminescence is a direct indication of the number of polaritons that are trapped at donors and acceptors. The preponderance of bound-exciton emission indicates that free-exciton trapping is much more important than radiative decay in determining the lifetime of the polariton. We will show below that most of the polariton trapping occurs from near the bottom of the polariton band.

IV. POLARITON LINE SHAPE

In this section we will examine the experimental polariton PL spectra and compare the line shapes to theoretical models of polariton luminescence. Sample-to-sample variations in the no-phonon emission as well as the different line shapes produced by the various polariton emission mechanisms will be considered. The polariton line shape will be shown to be determined primarily by polariton mobility and scattering.

Figure 3 illustrates the sample-to-sample variation in the no-phonon polariton PL at 1.5953 eV. These spectra show two lines at 1.5935 eV (DBE') and 1.5940 eV (DBE''), which are due to donor-bound excitons that are split from the principal DBE line by the electron-hole spin-exchange interaction within the bound exciton.²¹ The line at 1.5949 eV has been assigned to an excited state of the DBE by excitation spectroscopy²³ and the TET spectrum.²¹ This feature is in the proper position for the $n=2$ hydrogenic excited state of a DBE with a series limit at E_T . The no-phonon polariton emission falls in the region above 1.595 eV. Sample 1 [Fig. 3(a)] is the sample used for the PL spectrum of Fig. 2, and it is relatively pure. Sample 2 [Fig. 3(b)] contains substantial donor impurities, resulting in relatively intense DBE

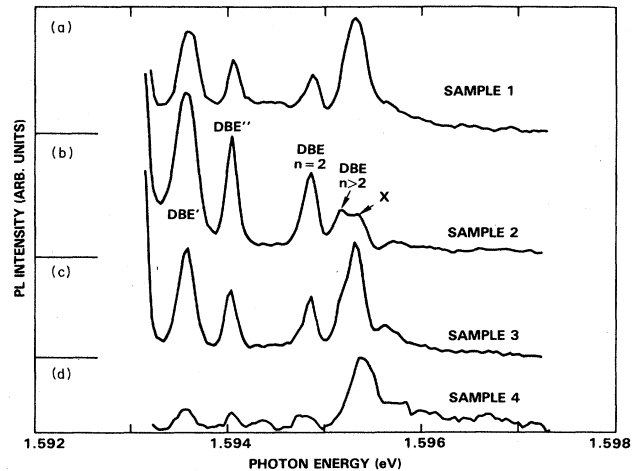


FIG. 3. Near-band-edge emission from four CdTe samples, showing variation in the polariton line shape. The peak assignments are explained in the text.

peaks. Sample 3 [Fig. 3(c)] has purity similar to that of sample 1, and the spectrum is nearly identical except for a slight dip at 1.5955 eV. Sample 4 [Fig. 3(d)] is from the same boule as sample 3, but it was not cadmium annealed, and thus is a sample with many acceptors and few donors. This is reflected in small excited DBE peaks and weak polariton emission.

In each of the spectra in Fig. 3, the polariton emission forms a broad band and a prominent peak near 1.5953 eV. In spectrum (b) there is a noticeable dip near 1.5955 eV, which is seen in varying degrees in the other three spectra. This dip falls at the minimum of the group velocity calculated from the dispersion curve of Fig. 1. This suggests that the line shape is influenced by polariton transport, as proposed by Koteles *et al.*^{12,28} (This is discussed in detail below.) The shape of the 1.5953-eV feature also shows large variations among the four spectra. Two possible assignments for the peak at 1.5953 eV are (1) polariton emission from below the bottleneck region, and (2) recombination of $n > 2$ DBE. If the DBE excited-state series limit is E_T , these two mechanisms will produce nearly identical photon energies.

The correlation of the DBE emission intensity with the shape of the band at 1.5953 eV makes it possible to assign the 1.5953-eV feature as a combination of partially overlapping bands from both excited DBE and polariton emission. Spectrum (b) has the greatest amount of DBE PL, and it also shows the largest PL amplitude at 1.5952 eV. Spectra (a) and (c), with much less DBE emission, have only a shoulder at 1.5952 eV. And spectrum (d), with very small DBE peaks, still has a substantial peak at 1.5953 eV. This indicates that the $n > 2$ DBE emission is not quite resolvable from the polariton emission, and it forms a shoulder on the main polariton peak at 1.5953 eV. Thus the 1.5953-eV emission is from the region of the polariton band just below the minimum in the group velocity. This assignment is very significant, since the 1.5953-eV peak represents a substantial amount of the no-phonon polariton PL.

The polariton emits luminescence through several different mechanisms, producing PL bands at several wavelengths. Comparison of the different PL line shapes yields additional insight into the PL mechanisms, in particular the no-phonon emission. Figure 4 shows four polariton emission bands, offset in photon energy to align the same polariton k states. (The LO-phonon energy, 21.2 meV, was determined by the difference between the ABE and ABE-LO peak energies.) These spectra were obtained from sample 5, which is similar to sample 2 in that the near-band-edge spectrum is dominated by DBE emission. The band shape that most accurately represents the quasithermal polariton distribution is the two-phonon replica in Fig. 4(d). In this wavelength region there is no reabsorption of PL, and the two-phonon emission process has equal luminescence probability for each k state.²⁹ The one-phonon replica [Fig. 4(c)] is broadened toward higher energies because the probability of PL emission in this band increases linearly with energy above the bottom of the band. The no-phonon polariton emission [Fig. 4(a)] is similar to the spectrum of the donor-rich sample in Fig. 3(b). This spectrum also shows a slight dip near the polariton group-velocity minimum. Figure 4(b) shows the two-electron transition (TET) region, which is relatively strong due to the high donor concentration.

Comparison of the phonon replicas of the polariton band with the no-phonon line shows that the bulk of the polariton population is at and just above the dip in the no-phonon band. Thus, this dip corresponds to the bottleneck region for polariton relaxation as well as the flattest part of the polariton dispersion.

Examination of the TET region of the spectrum supports the above assignment of the 1.5953-eV feature to polariton emission. A broad band at a shifted energy of 1.5958 eV corresponds to the peaks in the polariton replica spectra, and peaks also correspond to each of the no-phonon DBE peaks. A peak also corresponds to the 1.5952-eV shoulder, supporting the assignment as $n > 2$

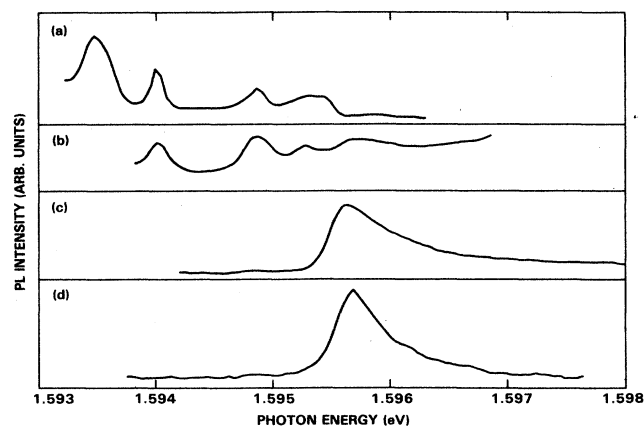


FIG. 4. Polariton emission line shapes from sample 5: (a) no-phonon line; (b) TET region; (c) LO-phonon replica; (d) 2LO-phonon replica. Spectra (b), (c), and (d) were shifted by 10.77, 21.2, and 42.4 meV, respectively, to align regions with the same k states.

DBE. But there is no peak corresponding to the 1.5953-eV feature, indicating that this is not DBE emission.

Our conclusion is that the 1.5953-eV feature is due to polariton emission from the sparsely populated region of the polariton band below the bottleneck. The no-phonon emission probability of these polaritons is enhanced because of their large group velocity and substantial photonlike character. In the remainder of this section we compare these results with proposed models of polariton emission.

Several models of polariton line shapes in various materials have been developed. Polariton PL lines have been observed with a variety of shapes; the line can vary among different samples of the same material, with sample preparation, or even with excitation power. Many materials, such as CdS, CdSe, and CuCl, have a polariton emission band with a single peak plus a shoulder on the high-energy side.¹⁹ Other semiconductors, such as GaAs and ZnTe, exhibit an asymmetric double peak. A unified theory to explain this diversity of behavior has proven elusive, but the existing theories can be divided into three groups: (1) The upper and lower polariton branches emit separately, leading to double peaks or shoulders,³⁰ (2) the emission is almost exclusively due to the lower polariton branch, but the surface transmission probability is modified by the upper branch,¹⁰ (3) the line shape is distorted by interactions of polaritons or photons with the crystal.^{7,11,12}

The first approach fails to predict the proper positions and the energy separation of the upper and lower polariton peaks, and cannot account for sample-to-sample variations in the spectra. The second theory has successfully fitted the line shapes of materials exhibiting single peaks with shoulders by assuming additional boundary conditions⁶ needed to calculate the surface transmission probabilities. In this model the polaritons are assumed to be homogeneously distributed in the crystal. This theory is not suitable for fitting the double-peaked spectra found in GaAs, ZnTe, or CdTe.

The third theory attempts to fit the double-peaked spectra by considering a nonhomogeneous distribution of polaritons interacting with the crystal. The crystal interaction can be called either "reabsorption" or scattering, since in the polariton picture the absorption of light resonant with polaritons actually consists of polariton scattering. The complementary process of photon emission occurs only after a polariton migrates to the crystal surface. A variety of experiments (primarily in GaAs) have implied the existence of a surface layer depleted of polaritons, and that transport of polaritons across this layer to the surface plays an important role in determining the line shape. (The line shape of the DBE can also be distorted by this layer.^{31,32}) Minima in polariton group velocities, and concurrent maxima in scattering probabilities, occur in the flattest part of the polariton dispersion just above the bottleneck, and it is this region that has been identified with the dip in the polariton spectra.

Detailed calculations of polariton line shapes in GaAs based on the impurity-scattering model have been performed by Lee *et al.*³³ using partial-wave analysis. They

found that neutral-donor scattering is the dominant scattering mechanism, due to the low donor ionization energy and the large spatial extent of neutral-donor wave functions. The calculations show that the polariton-scattering cross section *increases* as the group velocity *decreases*. The resulting polariton line shape depends on the assumed spatial distribution of polaritons in the sample, but the major result is that a dip in the polariton spectrum can occur at a photon energy corresponding to the minimum in the polariton group velocity. In GaAs the observed dips in the polariton line can be fitted by the impurity-scattering model.³³ Confirming this view, the dip in the GaAs polariton spectrum has been observed to disappear for very pure crystals,²⁸ passivated crystals,^{11,34} and just after an excitation pulse.¹²

Our data also show a dip for some samples, and the location of the dip matches the calculated position of the group-velocity minimum [Fig. 1(b)]. The fit of the velocity minimum with the observed dip in our polariton spectra is very good, and indicates that the impurity-scattering model is a proper description for polariton luminescence in CdTe. The major difference between our spectra and the GaAs spectra previously reported²⁸ is the greater asymmetry in the CdTe line, with much more PL coming from the polariton band below the velocity minimum. This could be explained by a weaker bottlenecking effect in CdTe.

In summary, both the sample-to-sample variation in the no-phonon line and the comparison of different polariton replica lines show that substantial no-phonon polariton emission occurs from the region just below the bottleneck in the dispersion curve. The X-LO and X-2LO polariton replicas show that the polariton population in this region is very small. The enhanced radiative efficiency of polaritons below the bottleneck is due to the high mobility and low scattering cross section for these polaritons. This viewpoint is in agreement with previous theories for the double-peaked polariton line observed in GaAs.^{12,28}

V. POLARITON INTRABAND RELAXATION

The prominent polariton emission in high-quality CdTe crystals is very useful for studying the dynamics of polariton formation and relaxation. Polaritons formed by optical excitation above the band gap have a wide distribution of energies and subsequently relax toward the bottleneck in the dispersion curve. The rate of acoustic-phonon scattering is greater than the polariton decay rate, which allows the polariton population to reach a quasiequilibrium with the lattice temperature. The polariton formation and relaxation processes have been studied in CdS,^{3,15} CdSe,^{3,16} and ZnTe,^{17,18} but questions remain about the formation and relaxation mechanisms. In particular, the possibility of delayed formation of polaritons from free electrons and holes has not been considered.

Experimental excitation of high-quality CdTe crystals was accomplished using picosecond optical pulses. Time-resolved PL was observed at several wavelengths within the X-LO band covering 2 meV of the polariton dispersion at and above the bottleneck region. These

studies were performed at low excitation fluxes (2×10^{11} photons/pulse cm^2) to minimize nonlinear effects. The sample displaying the longest polariton lifetime (no. 1, $\tau > 7$ ns) was selected for these experiments to facilitate separation of effects due to polariton formation and intraband relaxation processes from those due to trapping and recombination of the polaritons.

Our results indicate that the polariton-formation process plays a major role in determining the time-resolved PL waveforms. Polaritons can be formed either by direct photon absorption or from the combination of an electron and a hole. If the optical excitation is resonant with the polariton band and below the band-gap energy, direct photon absorption will be the only formation mechanism and the formation rate will follow the excitation rate. In our experiments, however, we excite with photons well above the band gap, and many polaritons will be created from the photoexcited free electrons and holes.²⁰ This will lead to polariton formation that will persist with the lifetime of the free carriers, which can be several nanoseconds. However, formation of polaritons from free carriers is restricted to regions where the conduction and valence bands have equal group velocities, such as occurs near $\mathbf{k}=0$.³⁵ Thus polariton formation may be delayed until the carriers have relaxed to near $\mathbf{k}=0$. Electrons and holes can have different relaxation rates; so both the electron and hole relaxation processes are very important in determining the formation rate of polaritons.

Although the carrier-relaxation rates in CdTe have not been studied, considerable work has been done to determine the rates of electron and hole relaxation in GaAs.^{36,37} Carrier relaxation in CdTe will be similar to that in GaAs, although the acoustic-phonon coupling is weaker by about a factor of 2 because of the lower acoustic velocity.³⁸ For carriers created well above the band gap, the initial relaxation occurs through the emission of LO phonons. Within a few picoseconds the carriers have relaxed to within one LO-phonon energy of the band edge, and subsequent energy loss is through acoustic-phonon emission. This final thermalization with the lattice is relatively slow (nanosecond time scale), and it is this relaxation that will directly affect the polariton-formation rate in the region we have studied.

The decays of polariton emission as a function of time for several wavelengths within the LO-phonon replica band are shown in Fig. 5. The polaritons with energies well above the transverse exciton energy E_T show a rapid population buildup with a sharp transient spike, whereas the polaritons near E_T show a more gradual rise in population. These dramatic differences in the decay waveform across the band indicate that the emission spectrum is changing with time. Using decay waveforms from 11 wavelengths across the band, the data were transformed to show the time evolution of the polariton spectrum after the excitation pulse. These are shown in Fig. 6. During the excitation pulse ($t=0$ ns), polaritons are preferentially formed well above the bottom of the band, producing a band with no well-defined peak. At later times the polariton population forms a quasithermal distribution above the polariton bottleneck, leading to a PL spec-

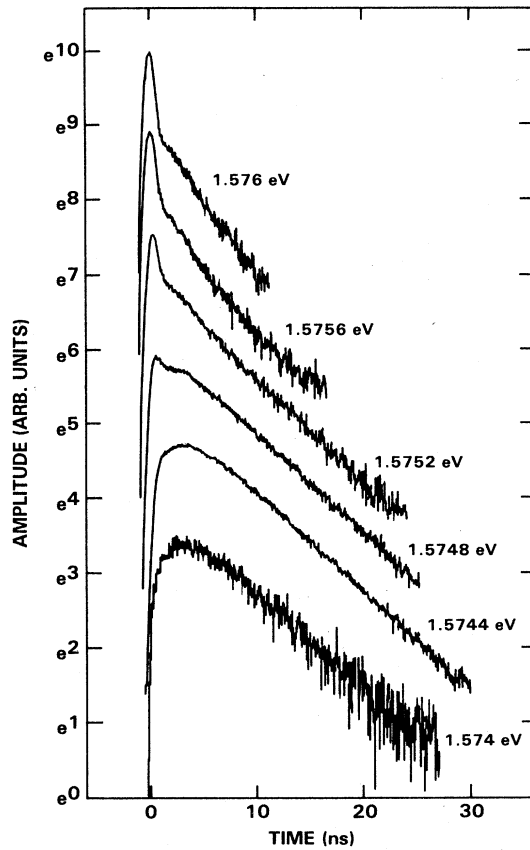


FIG. 5. Semilogarithmic plot of the time-resolved PL for sample 1 at various positions in the LO-phonon replica of the polariton band (X -LO) at 2 K. The decays are offset vertically by arbitrary amounts, and the detected photon energy in eV is labeled near each curve.

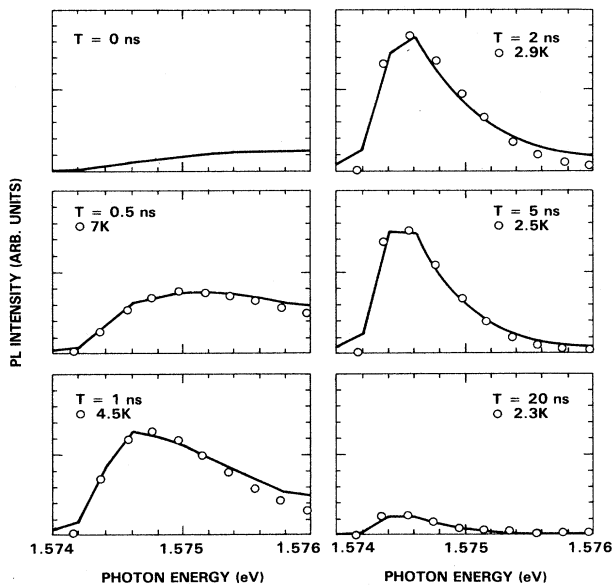


FIG. 6. Time-resolved spectra of the X -LO band derived from PL decay waveforms obtained at 11 wavelengths across the band. Open circles represent fits to a thermal distribution.

trum $I(E)$ that can be characterized by a thermal distribution:²⁹

$$I(E) = A(E - E_0)^{3/2} \exp[-(E - E_0)/kT], \quad (3)$$

where A is a constant and E_0 is the energy of the bottom of the band. Equation (3) will be correct for low excitation densities and parabolic bands, and incorporates the wave-vector dependence of the emission probability from the LO-phonon sideband. The best fits of Eq. (3) to the time-resolved spectra are plotted in Fig. 6 (open circles). In general, the spectra could be fitted for about 1 meV above the bottom of the band, but above this the fitted curves dropped off too steeply, indicating that the polariton population does not correspond to a quasithermal equilibrium. Nonetheless, the fits show considerable cooling of the polariton population. At 0.5 ns, the polariton temperature is approximately 7 K, well above the lattice temperature. By 2 ns the polariton temperature has cooled to 2.9 K, after which the polariton temperature continues to slowly approach the lattice temperature. The final spectrum at 20 ns shows that the polariton temperature has cooled to 2.3 K, nearly equal to the lattice temperature. Furthermore, the fit to Eq. (3) is quite good, indicating that the polaritons have finally reached thermal equilibrium.

When the spectra in Fig. 6 are renormalized to remove the effect of the k -dependent emission rate,²⁹ they show the polariton band population as it changes in time. The time-dependent spectra $I(E)$ were divided by $E - E_0$, where $E_0 = 1.57416$ eV is the "band-bottom" energy used in the thermal distribution fits to Eq. (3). (This value of E_0 agrees well with $E_T - E_{LO} = 1.5742$ eV.) Due to the nonparabolic polariton dispersion (Fig. 1), this correction is not valid near E_0 , but it does provide additional insight into the polariton relaxation. The temporal behavior of the total polariton population was not sensitive to the choice of E_0 . The time-dependent population distributions are shown in Fig. 7. At times less than 0.5 ns the polariton populations are increasing at all observed energies. However, from $t = 0.5$ to 1 ns, the population at the top of the band is nearly constant, while the population near E_T is rapidly increasing.

This behavior is inconsistent with polariton cooling through acoustic-phonon emission with a rate that is constant or decreases with decreasing polariton k state. Such cooling mechanisms would produce a shifting of the polariton population toward the bottleneck, and the population at the top of the band would decrease. A plausible explanation for the observed behavior is continued polariton formation between $t = 0.5$ and 1 ns, with polaritons near E_T being preferentially formed. This indicates that by $t = 1$ ns the electrons and holes that are forming polaritons have relaxed to near the band edge.

The substantial reduction in polariton temperature between $t = 0.5$ and 1 ns is caused by the formation of low-energy polaritons, not by the cooling of the existing high-energy polaritons. Thus this cooling rate is determined by the dynamics of the carriers and the polariton formation rate, not the polariton dynamics. After $t = 1$ ns a reduction in polariton population in high k states is

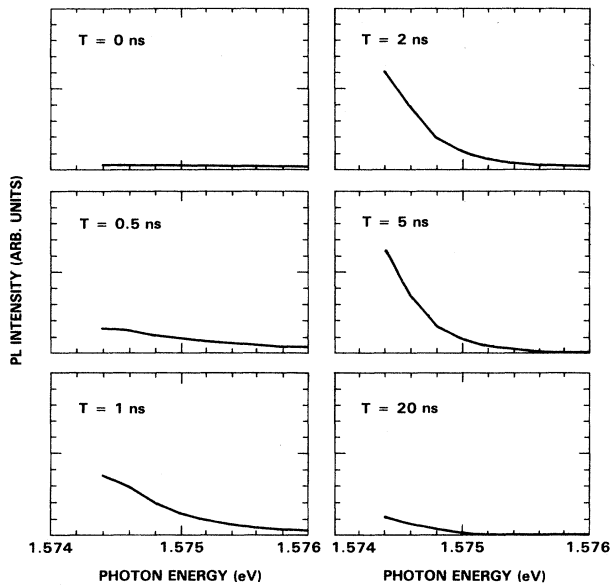


FIG. 7. Time-resolved polariton populations calculated by dividing spectra in Fig. 6 by the k -dependent emission probability. Because of uncertainties in the emission probability near the band bottom, these plots are truncated at 1.5744 eV.

seen, together with a continued buildup in population above the bottleneck. This is consistent with cooling through acoustic-phonon emission, but an analysis of the relaxation mechanisms producing the fast transient seen in the PL decay of high-energy polaritons shows that the initial reduction in population of these polaritons is actually due to polariton *dissociation*, not cooling.

An initial fast transient that peaks at about $t = 1.2$ ns is seen on decay waveforms for polaritons more than 1 meV above E_T . The decaying side of this transient occurs while the population at band bottom is still increasing, but an examination of the total polariton population (Fig. 8) shows that the total population is also decreasing at

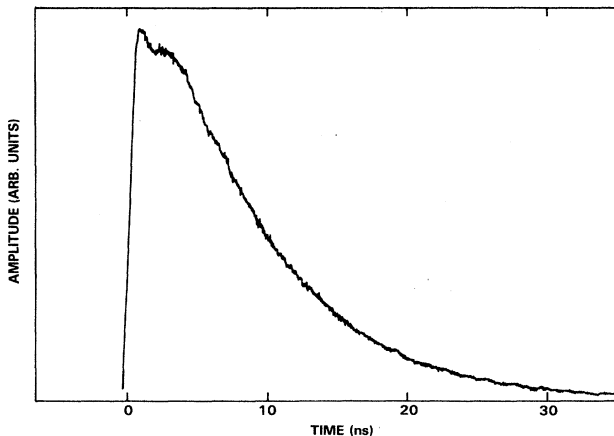


FIG. 8. Time dependence of total polariton population, calculated by integrating the normalized PL decay waveforms shown in Fig. 7.

this time. Figure 8 integrates the polariton population across the experimentally observed polariton band, and it shows that the total polariton population peaks at about $t = 1.4$ ns, then decreases until $t = 2.2$ ns, when it is followed by a slight increase to a broad peak at about $t = 3$ ns. The decrease in total population from $t = 1.4$ to 2.2 ns corresponds to the decaying side of the fast transient seen in the high-energy polariton waveforms, and it shows that these polaritons are not merely relaxing to lower k states. Thus, from $t = 1.4$ to 2.2 ns the formation of polaritons at band bottom is more than offset by the loss of population higher in the band, indicating that the high-energy polaritons are being destroyed. The subsequent slight rise in polariton population indicates that polaritons are still being formed from free electrons and holes as late as $t = 3$ ns, while the loss of high-energy polaritons has subsided.

Because of the initial fast transient, the decay waveforms for high-energy polaritons cannot be fit by a simple function that assumes constant formation and decay rates. A mechanism that could produce a variable relaxation rate is population thermalization due to polariton scattering by charged carriers. The possibility of interparticle scattering was investigated by varying the excitation intensity. The results for 1.5752-eV emission are shown in Fig. 9, with the excitation intensity varied from 10^{11} to 1.7×10^{12} photons/pulse cm^2 . At the highest exci-

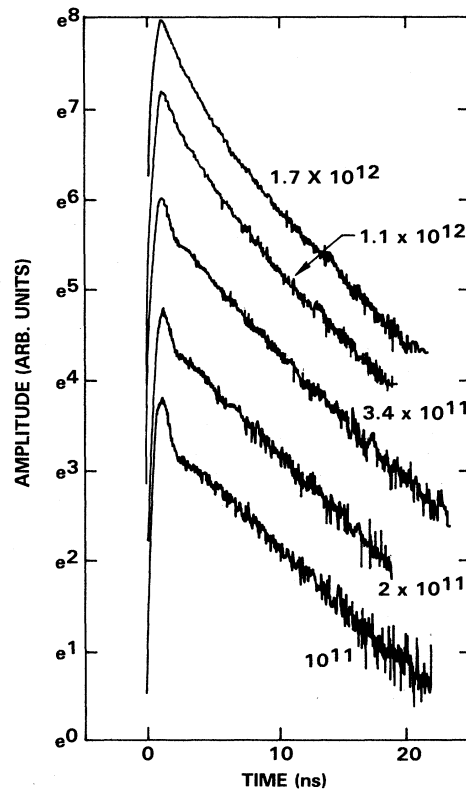


FIG. 9. Semilogarithmic plot of the excitation power dependence of PL decay from the X -LO band at 1.5752 eV. The excitation power in units of photons/pulse cm^2 is labeled near each decay.

tation powers, the risetime of the PL waveform is unchanged, but the trailing side of the initial transient shows a longer lifetime. (This waveform can be fit reasonably well by a model waveform with one rising and two decaying components.) Thus the polariton relaxation rate is lower at higher excitation densities, which indicates that carrier scattering does not lead to the fast polariton relaxation.

We believe that the variation in the polariton relaxation rate is produced by a relaxation channel out of the polariton state that becomes saturated. A plausible candidate is the dissociation of a polariton by an ionized acceptor. The field around such a center would cause the electron and hole within the polariton to experience forces in opposite directions. In addition, the binding energy of a hole to the acceptor (> 50 meV) is much greater than the polariton binding energy (10 meV). Thus a polariton passing close to an ionized acceptor would readily produce a neutral acceptor and a free electron. Such a relaxation mechanism would become saturated when all the available acceptors were neutralized by polaritons or free holes. At high excitation densities this would occur very rapidly, and this relaxation channel would become negligible. Thus the dissociation of polaritons by ionized acceptors can explain both the initial transient observed on PL waveforms at low excitation densities and the changes in this transient as the excitation level is increased. Ionized acceptors are abundant in heavily compensated semiconductors such as CdTe. Since this is not an intrinsic process, the importance of this mechanism will vary from sample to sample. However, it is significant that the fast transients are seen in our purest samples.

In summary, the dynamics of exciton polariton formation and relaxation are complex. The total polariton population shows a rapid rise in the first nanosecond after excitation, followed by small changes for the next two nanoseconds. From about $t=1.2$ to 2.2 ns the high-energy polaritons show a rapid decrease in population that cannot be explained by cooling, and is probably due to polariton dissociation. The total polariton population remains high due to continued polariton formation from electrons and holes as late as $t=3$ ns. This delayed formation occurs near E_T , in contrast to the initial polariton formation, which is spread across the band. This change in the energy of polaritons being formed is due to the relaxation of the free carriers, and is responsible for much of the reduction in the polariton temperature seen in the first 3 ns. The cooling of the polariton population through acoustic-phonon emission is much slower, and requires about 20 ns to produce a fully thermalized distribution.

VI. BOUND-EXCITON DYNAMICS

In samples with free-exciton lifetimes in the range of 3–7 ns, the observed temporal waveforms produced by bound-exciton radiative recombination have decay lifetimes approximately equal to that of the free-exciton population. This effect has been previously observed in other II-VI compound semiconductors,³⁹ and is the result of

the bound-exciton lifetime being shorter than the free-exciton lifetime. Population does not accumulate in the bound-exciton levels, and the rise and fall of the bound-exciton population follows that of the free-exciton population. This situation has been previously analyzed for the case of an instantaneous rise and exponential decay in the free-exciton population, which produces a waveform for bound-exciton emission that includes the bound-exciton lifetime as a risetime.³⁹

$$P_B(t) = A [\exp(-t/\tau_F) - \exp(-t/\tau_B)], \quad (4)$$

where A is a constant, $P_B(t)$ is the bound-exciton population, τ_B is the bound-exciton lifetime, and τ_F is the free-exciton lifetime. Although Eq. (4) has been successfully fitted to bound-exciton decays in other materials, attempts to fit our bound-exciton-decay data to Eq. (4) were not successful in many cases, and we have developed a model for bound-exciton decays that is valid for arbitrary free-exciton populations.

As discussed above, the observed temporal waveforms for free-exciton PL emission have risetimes substantially longer than our instrumental response. Thus Eq. (4) must be modified to reflect the noninstantaneous rise in the population feeding in to the bound state. We require a solution to the differential equation of the bound-exciton population with arbitrary free-exciton population $P_F(t)$:

$$\frac{d}{dt}P_B(t) = k_T P_F(t) - \frac{1}{\tau_B} P_B(t), \quad (5)$$

where k_T is the rate constant for the binding of free excitons. The solution is the convolution of an exponential decay $\exp(-t/\tau_B)$ with the function representing the rate at which population enters the bound-exciton state, $k_T P_F(t)$:

$$P_B(t) = \int_0^t e^{-(t-x)/\tau_B} k_T P_F(x) dx. \quad (6)$$

The bound-exciton lifetime τ_B is determined by choosing an experimentally measured polariton decay waveform $P_F(t)$ and varying τ_B in Eq. (6) to produce the best fit to the bound-exciton decay $P_B(t)$. This procedure produces an excellent fit to both the rising and decaying sides of the observed bound-exciton waveforms, and makes it possible to measure the bound-exciton lifetime in spite of the complexities of free-exciton intraband relaxation.

Figure 10 shows the PL decay of the ABE at 1.5892 eV (associated with the sodium acceptor) from sample 1 at 2 K. The data were fitted using both model waveforms above. By treating the polariton lifetime as an adjustable parameter, Eq. (4) produced a reasonable fit with $\tau_B = 3.5$ ns and $\tau_F = 6.7$ ns. However, interpreting this τ_F as the polariton lifetime conflicts with the observed polariton lifetime at the peak of the X-LO band of 7.7 ns. In fact, the actual ABE decay lifetime is 7.6 ns, but the 3.5-ns risetime parameter used for this fit lengthens the decaying side of the waveform. A significantly better fit ($\chi^2 = 2247$ versus 3533) is produced by Eq. (6) and is shown as the dotted line. This fit is produced by convolving a measured polariton decay waveform with a 2.1-ns exponential. Although both fits are close to the data, the

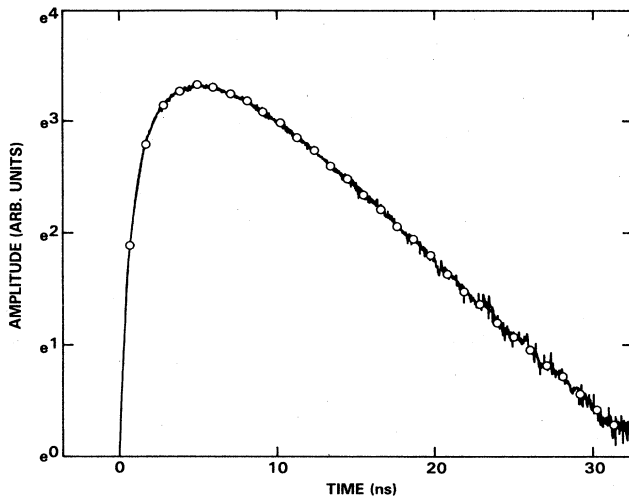


FIG. 10. Semilogarithmic plot of the time-resolved PL of excitons bound to neutral sodium acceptors (ABE at 1.5892 eV) in sample 1. The open circles represent the convolution of a measured polariton decay and an exponential with a 2.1-ns lifetime.

convolution fit is preferable because it requires one less adjustable parameter.

Although Eq. (6) provides an excellent fit to the bound-exciton decays, the quality of the fit depends upon which polariton decay waveform (Fig. 5) is used to represent the population feeding the bound exciton. This makes it possible to determine which regions of the polariton band are most likely to become bound at impurity sites. If the polariton band had a uniform binding rate, then the total polariton population (Fig. 8) would provide the feeding function to be used in Eq. (6). However, attempts to fit the ABE decay by convolutions using the total population waveform were unsatisfactory, due to the initial transient seen in the waveform in Fig. 8. Since this transient is produced by the polariton population at high energies in the band, the high-energy polaritons would appear to have a low trapping rate. In fact, the best fits are generated by convolving the ABE lifetime with polariton decays from near the bottom of the band, which have a risetime of about 1.8 ns. The polariton decays from 1.5745, 1.5743, and 1.5741 eV all gave reasonable fits, but the 1.5745-eV decay provided the lowest χ^2 (2247 versus about 2800 for the other two). Decays from higher in the band led to substantially poorer convolution fits. This suggests that polariton binding is most likely from just above the bottom of the band. This may be because the trapping cross section decreases with polariton velocity, but the polaritons at the bottom of the band do not have enough velocity to encounter many binding sites. Unfortunately, the bound-exciton lifetime needed for the convolution fit varies with the polariton decay waveform chosen. The best fit was obtained with a bound-exciton lifetime of 2.1 ns, but the two polariton waveforms from lower in the band both gave a lifetime of 1.8 ns. Without a definitive knowledge of the proper polariton waveform to use, this range must be considered as an uncertainty in the bound-exciton lifetime.

The temperature dependence of the polariton lifetime supports the hypothesis that trapping occurs primarily from the bottom of the band. As the temperature is raised from 2 to 4.2 K, the lifetime of the decaying side of the polariton waveforms increases from 7.7 to 9.0 ns. The lifetime at 9 K is 9.1 ns, and then decreases at higher temperatures. For a decay process to slow down at higher temperatures is very unusual, but it is easily explained by the shift of the polariton population into higher k states with lower trapping rates and longer lifetimes. Thus the temperature dependence of the polariton lifetime supports the assertion that the trapping rate for polaritons varies across the band. This situation will complicate any complete description of polariton dynamics.

In this section we have proposed a new approach to deriving the bound-exciton lifetime from the time-resolved PL. Because the polariton population at the bottom of the band has a complex temporal profile with a finite risetime, the bound-exciton decays must be fitted to a convolution [Eq. (6)] of the polariton decays and an exponential decay representing the bound-exciton lifetime. The resulting fits are better than simple fits [Eq. (4)] to rising and decaying lifetimes, and do not involve treating the polariton lifetime as an adjustable parameter. Substantial uncertainty in the fitted bound-exciton lifetimes is due to an uncertainty in the portion of the polariton band that is trapping to become bound excitons. Clearly, however, the population feeding the bound exciton is from states near the bottom of the band.

VII. CONCLUSION

We have presented new evidence on excitonic polariton dynamics in CdTe, including polariton formation, intra-band relaxation, and decay. Analysis of our data leads to a number of conclusions concerning exciton polariton dynamics.

(1) In high-quality CdTe crystals substantial no-phonon polariton emission occurs from the sparsely populated region just below the bottleneck, which shows that transport effects dominate the no-phonon line shape. This is similar to the situation in GaAs.

(2) Both the formation and relaxation rates of polaritons vary with time and k state. Delayed polariton formation (until at least $t = 3$ ns) from relaxed electrons and holes is important, and contributes to the apparent cooling of the polariton population. A decay channel that rapidly saturates produces the initial transient spike seen on decay waveforms from high-energy polaritons. This decay is probably due to dissociation by ionized centers. Polariton trapping is the dominant decay channel, and the trapping rate is highest just above E_T . These complexities will make modeling of the polariton dynamics very difficult.

(3) Bound-exciton decay can be represented by a convolution of the polariton decay with an exponential representing the bound-exciton lifetime. The bound-exciton lifetime can be extracted if the time dependence

of the relevant polariton population is known. The trapping rate of the polaritons varies with k state in an unknown fashion, leading to considerable uncertainty in the bound-exciton lifetimes.

Many unanswered questions remain, regarding particularly the intraband polariton relaxation dynamics. Hopefully the results for CdTe presented here will contribute

to an understanding of the general problem of exciton polariton dynamics in direct-band-gap semiconductors.

ACKNOWLEDGMENTS

The authors would like to acknowledge many fruitful discussions with J. Bajaj, and assistance from G. L. Bostrup, J. S. Chen, and S. H. Shin in sample preparation.

- ¹J. J. Hopfield, *Phys. Rev.* **112**, 1555 (1958).
- ²S. I. Pekar, *Zh. Eksp. Teor. Fiz.* **33**, 1022 (1957) [*Sov. Phys.—JETP* **6**, 785 (1958)].
- ³Farid Askary and Peter Y. Yu, *Phys. Rev. B* **31**, 6643 (1985).
- ⁴R. G. Ulbrich and C. Weisbuch, in *Festkörperprobleme XVIII—Advances in Solid State Physics*, edited by J. Treusch (Vieweg, Braunschweig, 1978), p. 217.
- ⁵E. L. Ivchenko, in *Excitons*, edited by E. I. Rashba and M. D. Sturge (North-Holland, Amsterdam, 1982), p. 141.
- ⁶Emil S. Koteles, in *Excitons*, edited by E. I. Rashba and M. D. Sturge (North-Holland, Amsterdam, 1982), p. 83.
- ⁷C. Weisbuch and R. G. Ulbrich, *J. Lumin.* **18/19**, 27 (1979).
- ⁸K. Aoki, T. Kinugasa, and K. Yamamoto, *Phys. Lett.* **72A**, 63 (1979).
- ⁹V. V. Travnikov and V. V. Krivolapchuk, *Fiz. Tverd. Tela (Leningrad)* **24**, 961 (1982) [*Sov. Phys.—Solid State* **24**, 547 (1982)].
- ¹⁰Farid Askary and Peter Y. Yu, *Solid State Commun.* **47**, 241 (1983).
- ¹¹L. Schulthies and C. W. Tu, *Phys. Rev. B* **32**, 6978 (1985).
- ¹²T. Steiner, M. L. W. Thewalt, E. S. Koteles, and J. P. Salerno, *Phys. Rev. B* **34**, 1006 (1986).
- ¹³Yutaka Toyozawa, *Prog. Theor. Phys. Suppl.* **12**, 112 (1959).
- ¹⁴Desmond V. O'Connor and David Phillips, *Time-Correlated Single Photon Counting* (Academic, New York, 1984).
- ¹⁵P. Weisner and U. Heim, *Phys. Rev. B* **11**, 3071 (1975).
- ¹⁶Yasuaki Masumoto and Shigeo Shionoya, *Phys. Rev. B* **30**, 1076 (1984).
- ¹⁷Y. Oka, K. Nakamura, and H. Fujisaki, *Phys. Rev. Lett.* **22**, 2857 (1986).
- ¹⁸A. Kurita, Y. Fujikawa and T. Kushida, *J. Lumin.* **38**, 70 (1987).
- ¹⁹P. J. Dean and D. C. Herbert, in *Excitons*, Vol. 14 of *Topics in Current Physics*, edited by K. Cho (Springer-Verlag, Berlin, 1979).
- ²⁰Donald E. Cooper, J. Bajaj, and P. R. Newman, *J. Cryst. Growth* **86**, 544 (1988).
- ²¹S. Suga, W. Dreybrodt, F. Willmann, P. Hiesinger, and K. Cho, *Solid State Commun.* **15**, 871 (1974).
- ²²P. Hiesinger, S. Suga, F. Willmann, and W. Dreybrodt, *Phys. Status Solidi B* **67**, 641 (1975).
- ²³A. Nakamura and C. Weisbuch, *Solid-State Electron.* **21**, 1331 (1978).
- ²⁴E. Cohen, R. A. Street, and A. Muranevich, *Phys. Rev. B* **28**, 7115 (1983).
- ²⁵J. L. Pautrat, J. M. Francou, N. Magnea, E. Molva, and K. Saminadayar, *J. Cryst. Growth* **72**, 194 (1985).
- ²⁶E. I. Rashba and G. E. Gurgenshvili, *Fiz. Tverd. Tela (Leningrad)* **4**, 1029 (1962) [*Sov. Phys.—Solid State* **4**, 759 (1962)].
- ²⁷C. H. Henry and K. Nassau, *Phys. Rev. B* **1**, 1628 (1970).
- ²⁸Emil S. Koteles, Johnson Lee, J. P. Salerno, and M. O. Vassell, *Phys. Rev. Lett.* **55**, 867 (1985).
- ²⁹S. Permogorov, in *Excitons*, edited by E. I. Rashba and M. D. Sturge (North-Holland, Amsterdam, 1982), p. 177.
- ³⁰S. Suga and T. Koda, *Phys. Status Solidi B* **66**, 255 (1974).
- ³¹H. Venghaus, *J. Lumin.* **16**, 331 (1978).
- ³²D. C. Reynolds, D. W. Langer, C. W. Litton, G. L. McCoy, and K. K. Bajaj, *Solid State Commun.* **46**, 473 (1983).
- ³³Johnson Lee, Emil S. Koteles, M. O. Vassell, and J. P. Salerno, *J. Lumin.* **34**, 63 (1985).
- ³⁴B. J. Skromme, C. J. Sandroff, E. Yablonovich, and T. Gmitter, *Appl. Phys. Lett.* **51**, 2022 (1987).
- ³⁵M. D. Sturge, in *Excitons*, edited by E. I. Rashba and M. D. Sturge (North-Holland, Amsterdam, 1982) p. 1.
- ³⁶R. G. Ulbrich, *Solid State Electron.* **21**, 51 (1978).
- ³⁷S. A. Lyon, *J. Lumin.* **35**, 121 (1986).
- ³⁸R. R. Nag, *Theory of Electrical Transport in Semiconductors* (Pergamon, Oxford, 1972).
- ³⁹F. Minami and K. Era, *Solid State Commun.* **53**, 187 (1985).